The reaction mechanism of SO_3 with the multifunctional compound ethanolamine and its atmospheric implications

Rui Wang [a], Ruxue Mu [a,‡], Zeyao Li [a,‡], Yongqi Zhang [a], Jihuan Yang [a], Guanhua Wang [a], Tianlei Zhang [a,*]

[a] *Institute of Theoretical and Computational Chemistry, Shaanxi Key Laboratory of Catalysis, School of Chemical & Environment Science, Shaanxi University of Technology, Hanzhong, Shaanxi, 723000, P. R. China*

* Corresponding authors. Tel: +86-0916-2641083, Fax: +86-0916-2641083.
E-mail: ztianlei88@l63.com (T. L. Zhang)
‡ Ruxue Mu and Zeyao Li have contributed equally to this work.

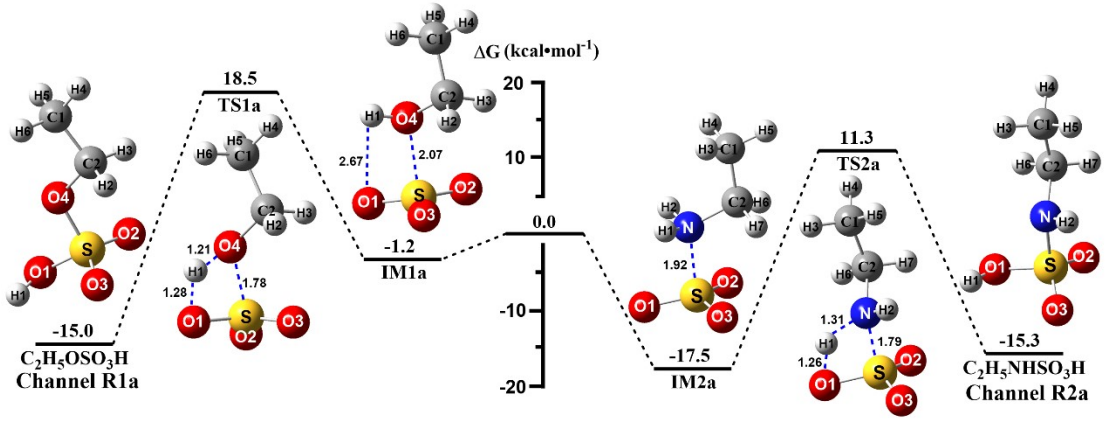

Fig. S1 Schematic potential energy surfaces for the reactions of SO_3 + C_2H_5OH and SO_3 + $C_2H_5NH_2$ at the CCSD(T)-F12/cc-pVTZ-F12//M06-2X/6-311++G(2*df*,2*pd*) level

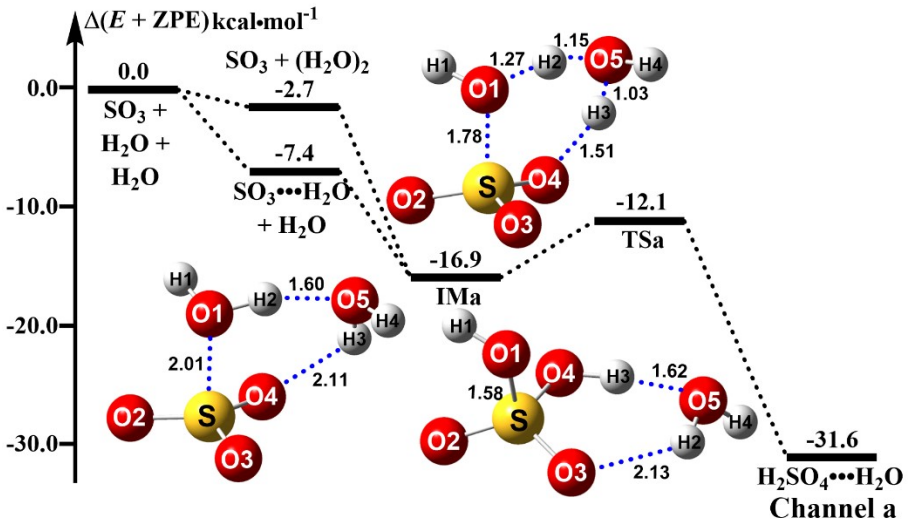

Fig. S2 Schematic potential energy surface for the reaction of SO_3 + $2H_2O$ at the CCSD(T)-F12/cc-pVTZ-F12//M06-2X/6-311++G(2*df*,2*pd*) level

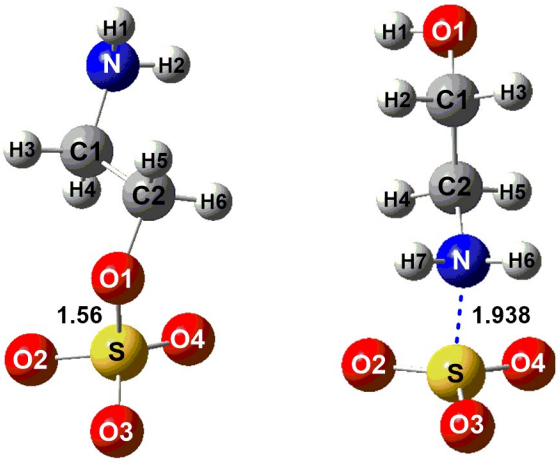

$NH_2CH_2CH_2OSO_3^-$ $HOCH_2CH_2NH_2^+\cdots SO_3^-$

Fig. S3 The optimized geometrical structures for $NH_2CH_2CH_2OSO_3^-$ and $HOCH_2CH_2NH_2^+\cdots SO_3^-$ ion at the M06-2X/6-311++G(2*df*,2*pd*) level

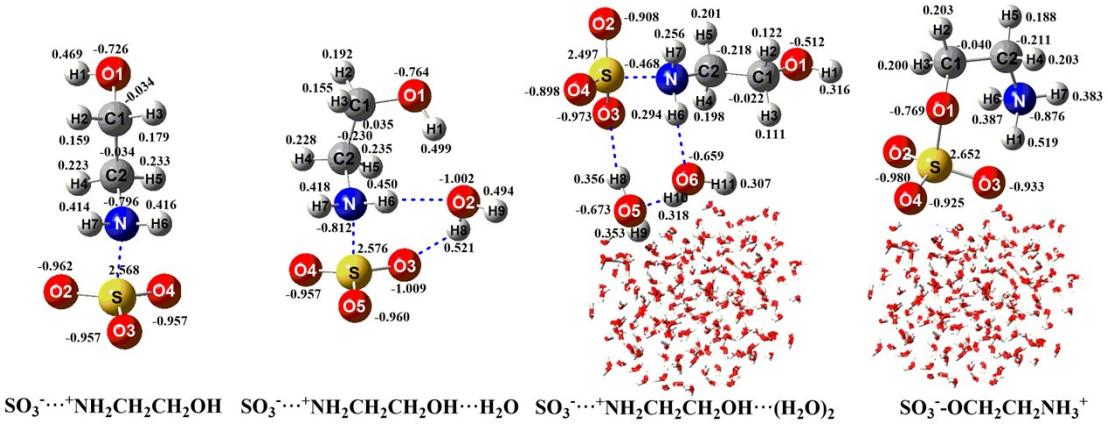

Fig. S4 NBO charges of $SO_3^{-}\cdots{}^{+}NH_2CH_2CH_2OH$ and $SO_3^{-}\cdots{}^{+}NH_2CH_2CH_2OH\cdots H_2O$ in the gas phase optimized at the M06-2X/6-311++G(2*df*,2*pd*) level and the NBO charges of ring complexes of $SO_3^{-}\cdots{}^{+}NH_2CH_2CH_2OH\cdots(H_2O)_2$ and SO_3^{-}-$OCH_2CH_2NH_3^{+}$ on the droplet optimized with ONIOM method (M06-2X/6-311++G(2*df*,2*pd*):pm6)

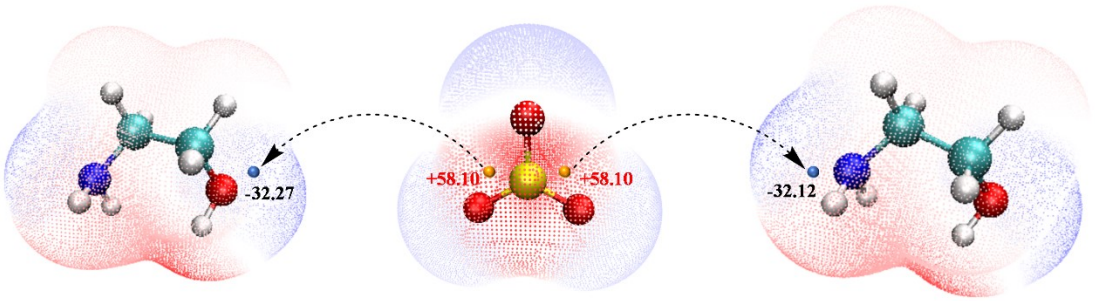

Fig. S5 Computed electrostatic potential mapped molecular van der Waals (vdW) surfaces of SO_3 with OH and NH_2 moieties $HOCH_2CH_2NH_2$ molecules at the M06-2X/6-311++G(2*df*,2*pd*) level

Table S1 The Energy barriers (ΔE) and unsigned error (UE) (kcal·mol^{-1}) for the SO_3 + $HOCH_2CH_2NH_2$ reaction at different theoretical methods with zero-point energy (ZPE) correction

Channel [a]	Methods	ΔE [b]	ΔE [c]	ΔE [d]	UE
Channel R1	CCSD(T)/CBS//M06-2X/ 6-311++G(2*df*,2*pd*)	-27.0	1.9	-24.8	0.00
	CCSD(T)-F12/cc-pVTZ-F12//M06-2X/ 6-311++G(2*df*,2*pd*)	-27.2	2.2	-24.5	0.27
	CCSD(T)/aug-cc-pVTZ//M06-2X/ 6-311++G(2*df*,2*pd*)	-25.7	2.4	-23.8	0.93
	CCSD(T)-F12/cc-pVDZ-F12//M06-2X/ 6-311++G(2*df*,2*pd*)	-25.8	3.5	-23.2	1.47
Channel R2	CCSD(T)/CBS//M06-2X/ 6-311++G(2*df*,2*pd*)	-15.8	6.0	-33.1	0.00
	CCSD(T)-F12/cc-pVTZ-F12//M06-2X/ 6-311++G(2*df*,2*pd*)	-15.6	6.3	-32.9	0.23
	CCSD(T)/aug-cc-pVTZ//M06-2X/ 6-311++G(2*df*,2*pd*)	-15.3	6.6	-31.6	0.87
	CCSD(T)-F12/cc-pVDZ-F12//M06-2X/ 6-311++G(2*df*,2*pd*)	-14.9	7.4	-31.5	1.23

[a] Channel R1 and Channel R2 denote the gas-phase reactions of SO_3 with OH and NH_2 moieties of MEA, respectively;

[b, c and d] respectively denote the species of pre-reactive complexes, transition states and products involved in the SO_3 + MEA reaction.

As presented in Table S1, the unsigned error at the CCSD(T)-F12/cc-pVDZ-F12//M06-2X/6-311++G(2*df*,2*pd*) level compared to unsigned error calculated at the CCSD(T)/CBS//M06-2X/6-311++G(2*df*,2*pd*) level, was more than 1.47 kcal·mol^{-1}, indicating that CCSD(T)-F12 with a small basis set of cc-pVDZ-F12 is not appropriate. As compared with unsigned error calculated at the CCSD(T)/CBS//M06-2X/6-311++G(2*df*,2*pd*) level, unsigned errors calculated at CCSD(T)/aug-cc-pVTZ//M06-2X/6-311++G(2*df*,2*pd*) and CCSD(T)-F12/cc-pVTZ-F12//M06-2X/6-311++G(2*df*,2*pd*) were 0.93 and 0.27 kcal·mol^{-1}, respectively, suggesting that the relative energies obtained at the CCSD(T)-F12/cc-pVTZ-F12//M06-2X/6-311++G(2*df*,2*pd*) level is the most favorable among three levels of CCSD(T)-F12/cc-pVDZ-F12//M06-2X/6-311++G(2*df*,2*pd*), CCSD(T)/aug-cc-pVTZ//M06-2X/6-311++G(2*df*,2*pd*) and CCSD(T)-F12/cc-pVTZ-F12//M06-2X/6-311++G(2*df*,2*pd*). Considering the computational accuracy, the CCSD(T)-F12/cc-pVTZ-F12//M06-2X/6-311++G(2*df*,2*pd*) method was chosen to calculate the single point energies of all species for the SO_3 + MEA reactions without and with water. So, the single-point energy

calculations for the SO_3 + MEA reaction without and with water molecule in the gas phase have been performed at the CCSD(T)-F12/cc-pVTZ-F12 level based on the optimized geometries at the M06-2X/6-311++G(2*df*,2*pd*) level.

Table S2 Relative energies (ΔE and $\Delta(E + ZPE)$/(kcal·mol^{-1})), enthalpies (ΔH/(kcal·mol^{-1})), entropy (S(298 K)/(cal·mol^{-1}·K^{-1})) and Gibbs free energies (ΔG(298 K)/(kcal·mol^{-1})) for the reaction of SO_3 with C_2H_5OH and $C_2H_5NH_2$, along with the reactions between SO_3 and the OH and NH_2 moieties of $HOCH_2CH_2NH_2$ without and with H_2O

Species	ZPE	ΔE	S	ΔG	$\Delta(E + ZPE)$	ΔH	T_1
$SO_3 + HOCH_2CH_2NH_2$	70.4	0.0	134.3	0.0	0.0	0.0	0.02820363
IM1	72.5	-17.7	94.5	-4.1	-15.6	-15.9	0.0144697
TS1	69.4	7.3	90.8	18.6	6.3	5.6	0.01471739
$NH_2CH_2CH_2SO_4H$	73.2	-35.6	86.4	-19.6	-32.9	-33.9	0.01397518
$SO_3 + NH_2CH_2CH_2OH$	70.4	0.0	134.3	0.0	0.0	0.0	0.02820363
IM2	73.7	-30.5	89.8	-14.6	-27.2	-27.9	0.01440033
TS2	70.0	2.6	91.6	14.2	2.2	1.5	0.01465095
$HOCH_2CH_2NHSO_3H$	72.5	-26.6	91.2	-12.2	-24.5	-25.0	0.01406416
$SO_3 + HOCH_2CH_2NH_2 + H_2O$	84.0	0.0	179.4	0.0	0.0	0.0	0.03820721
$SO_3\cdots H_2O + HOCH_2CH_2NH_2$	86.4	-9.8	147.5	1.5	-7.4	-8.0	0.02654947
$SO_3 + HOCH_2CH_2NH_2\cdots H_2O$	86.3	-6.0	149.5	4.7	-3.7	-4.2	0.0284588
IM_WM1	88.2	-27.5	106.5	-2.5	-23.3	-24.2	0.01394004
TS_WM1	86.4	-21.5	99.3	2.8	-19.1	-21.0	0.01392185
$NH_2CH_2CH_2SO_4H\cdots H_2O$	89.1	-44.7	99.9	-17.6	-39.6	-41.3	0.01359628
$SO_3 + NH_2CH_2CH_2OH + H_2O$	84.0	0.0	179.4	0.0	0.0	0.0	0.03820721
$SO_3\cdots H_2O + NH_2CH_2CH_2OH$	86.4	-9.8	147.5	1.5	-7.4	-8.0	0.02654947
$SO_3 + HOCH_2CH_2NH_2\cdots H_2O$	86.3	-6.0	149.5	4.7	-3.7	-4.2	0.0284588
IM_WM2	89.4	-43.2	105.0	-16.8	-37.8	-39.0	0.01396046
TS_WM2	86.4	-25.8	96.3	-1.0	-23.4	-25.7	0.01401585
$HOCH_2CH_2NHSO_3H\cdots H_2O$	88.4	-38.9	104.7	-13.5	-34.6	-35.8	0.01366066
$SO_3 + C_2H_5OH$	58.6	0.0	129.1	0.0	0.0	0.0	0.02786553
IM1a	60.9	-15.0	89.8	-1.2	-12.6	-12.9	0.01485214
TS1a	58.0	7.2	86.9	18.5	6.7	5.9	0.01506695
$C_2H_5SO_4H$	61.0	-29.3	87.6	-15.0	-26.8	-27.4	0.01418237
$SO_3 + C_2H_5NH_2$	66.7	0.0	129.5	0.0	0.0	0.0	0.02786553
IM2a	69.8	-32.2	88.8	-17.5	-29.1	-29.6	0.01438851
TS2a	66.6	-0.9	85.4	11.3	-1.0	-1.9	0.01474855
$C_2H_5NHSO_3H$	68.8	-29.4	87.5	-15.3	-27.3	-27.9	0.01400273

The schematic potential energy surfaces for the $SO_3 + HOCH_2CH_2NH_2$ reaction (in kcal·mol^{-1}) without (Fig. 1) and with (Fig. 2) water have been re-calculated at the CCSD(T)-F12/cc-pVTZ-F12//M06-2X/6-311++G(2*df*,2*pd*) level, whereas relative energies (ΔE and $\Delta(E + ZPE)$/(kcal·mol^{-1})), enthalpies (ΔH/(kcal·mol^{-1})), entropy (S(298 K)/(cal·mol^{-1}·K^{-1})) and Gibbs free energies (ΔG(298 K)/(kcal·mol^{-1})) for the reaction of SO_3 with C_2H_5OH and $C_2H_5NH_2$, along with the

reactions between SO_3 and the OH and NH_2 moieties of $HOCH_2CH_2NH_2$ without and with H_2O has been reorganized in Table S2.

Table S3 Equilibrium coefficients ($cm^3 \cdot molecule^{-1}$) for the $SO_3 \cdots H_2O$ and $HOCH_2CH_2NH_2 \cdots H_2O$ complexes within 212.6-320.0 K [a]

T/K	$SO_3 \cdots H_2O$	$HOCH_2CH_2NH_2 \cdots H_2O$
212.6	2.25×10^{-20}	1.99×10^{-23}
229.7	1.41×10^{-20}	1.58×10^{-23}
259.3	9.99×10^{-21}	1.33×10^{-23}
280.0	9.18×10^{-21}	1.28×10^{-23}
290.0	6.14×10^{-21}	1.05×10^{-23}
298.0	4.22×10^{-21}	8.75×10^{-24}
300.0	6.78×10^{-20}	3.45×10^{-23}
310.0	4.41×10^{-19}	8.84×10^{-23}
320.0	1.69×10^{-18}	1.75×10^{-22}

[a] All equilibrium coefficients were calculated by using energies computed at the CCSD(T)-F12/cc-pVTZ-F12//M06-2X/6-311++G(2*df*,2*pd*) level and partition functions obtained at the M06-2X/6-311++G(2*df*,2*pd*) level.

Table S4 Concentrations (molecules·cm^{-3}) for the $SO_3\cdots H_2O$ and $HOCH_2CH_2NH_2\cdots H_2O$ complexes within 212.6-320.0 K [a]

T/K	$SO_3\cdots H_2O$	$HOCH_2CH_2NH_2\cdots H_2O$
280.0	5.81	1.29×10^4
290.0	6.76	1.89×10^4
298.0	7.72	2.58×10^4
300.0	7.88	2.75×10^4
310.0	8.96	3.84×10^4
320.0	9.91	5.14×10^4

[a] All concentrations were calculated by using energies computed at CCSD(T)-F12/cc-pVTZ-F12//M06-2X/6-311++G(2*df*,2*pd*) level and partition functions obtained at the M06-2X/6-311++G(2*df*,2*pd*) level.

Table S5 Rate coefficients ($cm^3 \cdot molecule^{-1} \cdot s^{-1}$) for the SO_3 + $HOCH_2CH_2NH_2$ reaction without and with H_2O with HIR treatment calculated by master equation within 212.6-320.0 K [a]

Channel	Altitude (km)	T/K	with HIR treatments	without HIR treatments
Channel R1	0 km	280.0	1.58×10^{-18}	1.58×10^{-18}
		290.0	1.63×10^{-18}	1.63×10^{-18}
		298.0	1.67×10^{-18}	1.68×10^{-18}
		300.0	1.69×10^{-18}	1.69×10^{-18}
		310.0	1.75×10^{-18}	1.76×10^{-18}
		320.0	1.83×10^{-18}	1.84×10^{-18}
	5 km	212.6	1.68×10^{-18}	1.68×10^{-18}
	10 km	229.7	1.93×10^{-18}	1.93×10^{-18}
	15 km	259.3	2.40×10^{-18}	2.40×10^{-18}
Channel R2	0 km	280.0	1.51×10^{-16}	1.48×10^{-16}
		290.0	1.77×10^{-16}	1.74×10^{-16}
		298.0	1.99×10^{-16}	1.96×10^{-16}
		300.0	2.04×10^{-16}	2.01×10^{-16}
		310.0	2.33×10^{-16}	2.30×10^{-16}
		320.0	2.62×10^{-16}	2.60×10^{-16}
	5 km	212.6	1.50×10^{-16}	1.47×10^{-16}
	10 km	229.7	1.35×10^{-16}	1.31×10^{-16}
	15 km	259.3	1.65×10^{-16}	1.59×10^{-16}
Channel WM1	0 km	280.0	7.42×10^{-11}	4.46×10^{-11}
		290.0	7.53×10^{-11}	4.45×10^{-11}
		298.0	7.60×10^{-11}	4.43×10^{-11}
		300.0	7.62×10^{-11}	4.43×10^{-11}
		310.0	7.72×10^{-11}	4.40×10^{-11}
		320.0	7.78×10^{-11}	4.34×10^{-11}
	5 km	212.6	7.16×10^{-11}	4.41×10^{-11}
	10 km	229.7	6.68×10^{-11}	4.21×10^{-11}
	15 km	259.3	6.36×10^{-11}	4.02×10^{-11}
Channel WM2	0 km	280.0	5.85×10^{-12}	3.29×10^{-12}
		290.0	6.30×10^{-12}	3.50×10^{-12}
		298.0	6.65×10^{-12}	3.64×10^{-12}
		300.0	6.74×10^{-12}	3.67×10^{-12}
		310.0	7.17×10^{-12}	3.93×10^{-12}
		320.0	7.58×10^{-12}	4.51×10^{-12}
	5 km	212.6	6.45×10^{-12}	3.98×10^{-12}
	10 km	229.7	6.43×10^{-12}	4.31×10^{-12}
	15 km	259.3	6.32×10^{-12}	4.91×10^{-12}

[a] k_{R1} and k_{R2} were respectively denoted the rate coefficients for the reactions of SO_3 with OH and NH_2 moieties in $HOCH_2CH_2NH_2$; k_{WM1} and k_{WM2} were respectively denoted the rate coefficients for the reactions of SO_3 with OH and NH_2 moieties in $HOCH_2CH_2NH_2$ in the presence of H_2O.

As for the SO_3 + MEA reaction with water, the effect of HIR plays a minor role in the gas-phase reactions of SO_3 with OH (Channel WM1) and NH_2 (Channel WM2) moieties of MEA. As compared with the effect of HIR in Channels R1 and R2 without water, the effect of HIR in Channels WM1 and WM2 is further reduced. This can be explained as follows. On the one hand,

the pre-reactive complexes, products and transition states involved in the SO_3 + MEA reaction with water were shown the quasi-planar ring structures and cage-like ring structures. As compared with the naked reaction (Fig. 1), these ring structures reduce the ring tension obviously and increase the stability of the pre-reactive complexes, products and transition states greatly. On the other hand, the numbers of hydrogen bonds in H_2O-assisted pre-reactive complexes, products and transition states were increased, which hinder the rotation bonds of S-O1, H1-O5 and H8-O3 (Channel WM1) and S-N, H7-O5 and H8-O2 (Channel WM1) in H_2O-assisted pre-reactive complexes, products and transition states (Fig. 2).

Table S6 Rate coefficients ($cm^3 \cdot molecule^{-1} \cdot s^{-1}$) for the SO_3 + $HOCH_2CH_2NH_2$ reaction without and with H_2O calculated within 212.6-320.0 K [a]

Channels	Altitude (km)	0 km						5 km	10 km	15 km
	T (K)	280.0 K	290.0 K	298.0 K	300.0 K	310.0 K	320.0 K	259.3 K	229.7 K	212.6 K
Channel R1	k_{bR1}	1.73×10^{-18}	1.30×10^{-18}	1.09×10^{-18}	1.04×10^{-18}	8.94×10^{-19}	8.07×10^{-19}	4.18×10^{-18}	3.09×10^{-17}	1.72×10^{-16}
Channel R2	k_{bR2}	6.53×10^{-15}	3.52×10^{-15}	2.32×10^{-15}	2.10×10^{-15}	1.37×10^{-15}	9.63×10^{-16}	3.53×10^{-14}	1.10×10^{-12}	1.83×10^{-11}
Channel WM1	k_{bWM1}	6.49×10^{-5}	2.37×10^{-5}	1.12×10^{-5}	9.31×10^{-6}	3.89×10^{-6}	1.71×10^{-6}	6.95×10^{-4}	3.83×10^{-2}	0.68
Channel WM2	k_{bWM2}	9.08×10^{-2}	2.41×10^{-2}	8.94×10^{-3}	7.03×10^{-3}	2.22×10^{-3}	7.58×10^{-4}	2.08	4.23×10^{-2}	1.98×10^{-4}

[a] k_{bR1} and k_{bR2} were respectively denoted the rate coefficients for the reactions of SO_3 with OH and NH_2 moieties in $HOCH_2CH_2NH_2$ by the steady-state approximation; k_{bWM1} and k_{bWM2} were respectively denoted the rate coefficients for the reactions of SO_3 with OH and NH_2 moieties in $HOCH_2CH_2NH_2$ in the presence of H_2O by the steady-state approximation.

Part S1 Calculations of rate coefficients in the gas phase

The ILT methods [1,2] and RRKM theory [3,4] can be respectively expressed in equations (S1) and (S2), respectively.

$$k(\mathrm{T}) = \frac{1}{Q(\beta)} \int_0^\infty k(E)\rho(E)\exp(-\beta E)dE \tag{S1}$$

$$k(E) = \frac{W(E - E_0)}{h\rho(E)} \tag{S2}$$

Where $W(E\text{-}E_0)$ is the rovibrational sum of states at the optimized transition state (TS) geometry (excluding the degree of freedom associated with passage through the TS), E_0 is the reaction threshold energy, h is Planck's constant, ρ(E) is the active (ro-vibrational) density of state of the reactant at energy level E and $Q(\beta)$ is the corresponding canonical partition function. Meanwhile, Meanwhile, the tunneling effect was treated in RRKM calculation by employing a one-dimensional asymmetrical Eckart potential. The collisional energy-transfer process was computed with the temperature-dependent exponential-down model with $\left\langle \Delta E_{\mathrm{down}} \right\rangle = 75 \times \left(\frac{T}{300} \right)^{1.05}$ cm^{-1}, with N_2 as the bath gas [5,6]. The Lennard-Jones (L-J) parameters of epsilon ε/k_B = 218.1 K and sigma σ = 3.13 Å were used for SO_3, while the parameters of epsilon ε/k_B = 470.6 K and sigma σ = 4.41 Å were estimated for MEA.

References

[1] Kumar, A., Mallick, S., Kumar, P., Oxidation of HOSO by Cl: a new source of SO_2 in the atmosphere? *Phys. Chem. Chem. Phys.*, **2021**, *23*, 18707-18711.

[2] Horváth, G., Horváth, I., Almousa, S. A. D., Telek, M.,. Numerical inverse laplace transformation using concentrated matrix exponential distributions. *Perform. Evaluation*, **2020**, *137*, 102067.

[3] Mai, T. V. T., Duong, M. V., Nguyen, H. T., Huynh, L. K., Ab initio kinetics of the $HOSO_2 + {}^3O_2 \rightarrow SO_3 + HO_2$ reaction. *Phys. Chem. Chem. Phys.* **2018**, *20*, 6677-6687.

[4] Mallick, S., Kumar, A., Kumar, P., Oxidation of HOSO by NH_2: A new path for the formation of an acid rain precursor. *Chem. Phys. Lett.* **2021**, *773*, 138536.

[5] Mai, T. V. T.; Nguyen, H. T.; Huynh, L. K. J. P. C. C. P., Ab initio dynamics of hydrogen abstraction from N_2H_4 by OH radicals: an RRKM-based master equation study. *Phys. Chem. Chem. Phys.* **2019,** *21*, (42), 23733-23741.

[6] Mai, T. V. T.; Nguyen, H. T.; Huynh, L. K. J. A. E., Kinetics of hydrogen abstraction from CH_3SH by OH radicals: An ab initio RRKM-based master equation study. *Atmos. Environ.* **2020,** *242*, 117833.

Table S7 The high-pressure limiting rate coefficients ($cm^3 \cdot molecule^{-1} \cdot s^{-1}$) for the reaction of SO_3 with C_2H_5OH and $C_2H_5NH_2$, along with the reactions between SO_3 and the OH and NH_2 moieties of $HOCH_2CH_2NH_2$ without and with H_2O within 212.6-320.0 K

T (K)	$SO_3 + HOCH_2CH_2NH_2 \rightarrow SO_3\cdots HOCH_2CH_2NH_2$	$SO_3 + HOCH_2CH_2NH_2 \rightarrow SO_3\cdots NH_2CH_2CH_2OH$	$SO_3 + HOCH_2CH_2NH_2 + H_2O \rightarrow SO_3\cdots HOCH_2CH_2NH_2\cdots H_2O$
212.6	6.74×10^{-11}	6.20×10^{-11}	4.52×10^{-11}
229.7	7.01×10^{-11}	6.45×10^{-11}	4.69×10^{-11}
259.3	7.44×10^{-11}	6.84×10^{-11}	4.98×10^{-11}
280.0	7.73×10^{-11}	7.11×10^{-11}	5.18×10^{-11}
290.0	7.87×10^{-11}	7.24×10^{-11}	5.27×10^{-11}
298.0	7.98×10^{-11}	7.34×10^{-11}	5.34×10^{-11}
300.0	8.00×10^{-11}	7.36×10^{-11}	5.36×10^{-11}
310.0	8.13×10^{-11}	7.48×10^{-11}	5.45×10^{-11}
320.0	8.23×10^{-11}	7.60×10^{-11}	5.54×10^{-11}

T (K)	$SO_3 + HOCH_2CH_2NH_2 + H_2O \rightarrow SO_3\cdots NH_2CH_2CH_2OH\cdots H_2O$	$SO_3 + C_2H_5OH \rightarrow SO_3\cdots C_2H_5OH$	$SO_3 + C_2H_5NH_2 \rightarrow SO_3\cdots C_2H_5NH_2$
212.6	5.95×10^{-11}	8.06×10^{-11}	5.24×10^{-11}
229.7	6.18×10^{-11}	8.37×10^{-11}	5.45×10^{-11}
259.3	6.56×10^{-11}	8.89×10^{-11}	5.78×10^{-11}
280.0	6.82×10^{-11}	9.24×10^{-11}	6.01×10^{-11}
290.0	6.94×10^{-11}	9.40×10^{-11}	6.12×10^{-11}
298.0	7.04×10^{-11}	9.53×10^{-11}	6.20×10^{-11}
300.0	7.06×10^{-11}	9.56×10^{-11}	6.22×10^{-11}
310.0	7.18×10^{-11}	9.72×10^{-11}	6.32×10^{-11}
320.0	7.29×10^{-11}	9.88×10^{-11}	6.42×10^{-11}

Table S8 Rate coefficients ($cm^3 \cdot molecule^{-1} \cdot s^{-1}$) for the reaction of SO_3 with C_2H_5OH, $C_2H_5NH_2$ and $2H_2O$ calculated by master equation within 212.6-320.0 K [a]

Catalysts	Altitude (km)	0 km						5 km	10 km	15 km
	T (K)	280.0 K	290.0 K	298.0 K	300.0 K	310.0 K	320.0 K	259.3 K	229.7 K	212.6 K
Channel R1a	k_{R1a}	5.46×10^{-18}	5.63×10^{-18}	5.81×10^{-18}	5.86×10^{-18}	6.16×10^{-18}	6.54×10^{-18}	5.58×10^{-18}	6.27×10^{-18}	7.41×10^{-18}
Channel R2a	k_{R2a}	2.89×10^{-15}	3.52×10^{-15}	4.10×10^{-15}	4.25×10^{-15}	5.07×10^{-15}	5.97×10^{-15}	3.11×10^{-15}	2.89×10^{-15}	3.87×10^{-15}
Channel a	k_a	3.22×10^{-12}	2.79×10^{-12}	2.48×10^{-12}	2.41×10^{-12}	2.09×10^{-12}	1.81×10^{-12}	4.24×10^{-12}	6.32×10^{-12}	7.81×10^{-12}

[a] k_{R1a}, k_{R2a} and k_a was respectively denoted the rate coefficients for the $SO_3 + C_2H_5OH$, $SO_3 + C_2H_5NH_2$ and $SO_3 + 2H_2O$ reactions.

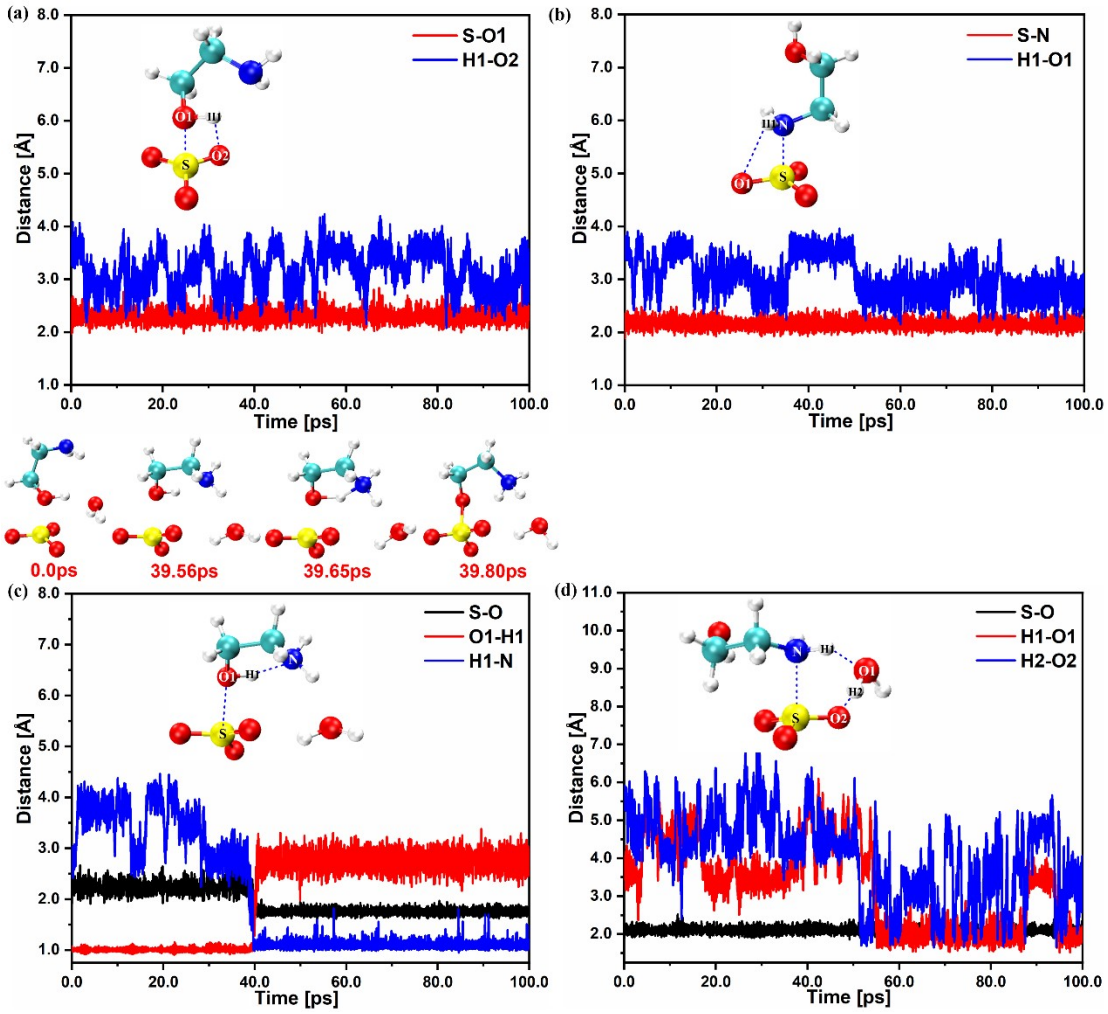

Fig. S6 The dynamic trajectories of the gas-phase reaction of SO_3 with OH and NH_2 moieties of MEA without and with H_2O (The white, red, yellow, gray and blue spheres represent H, O, S, C and N atoms, respectively.)

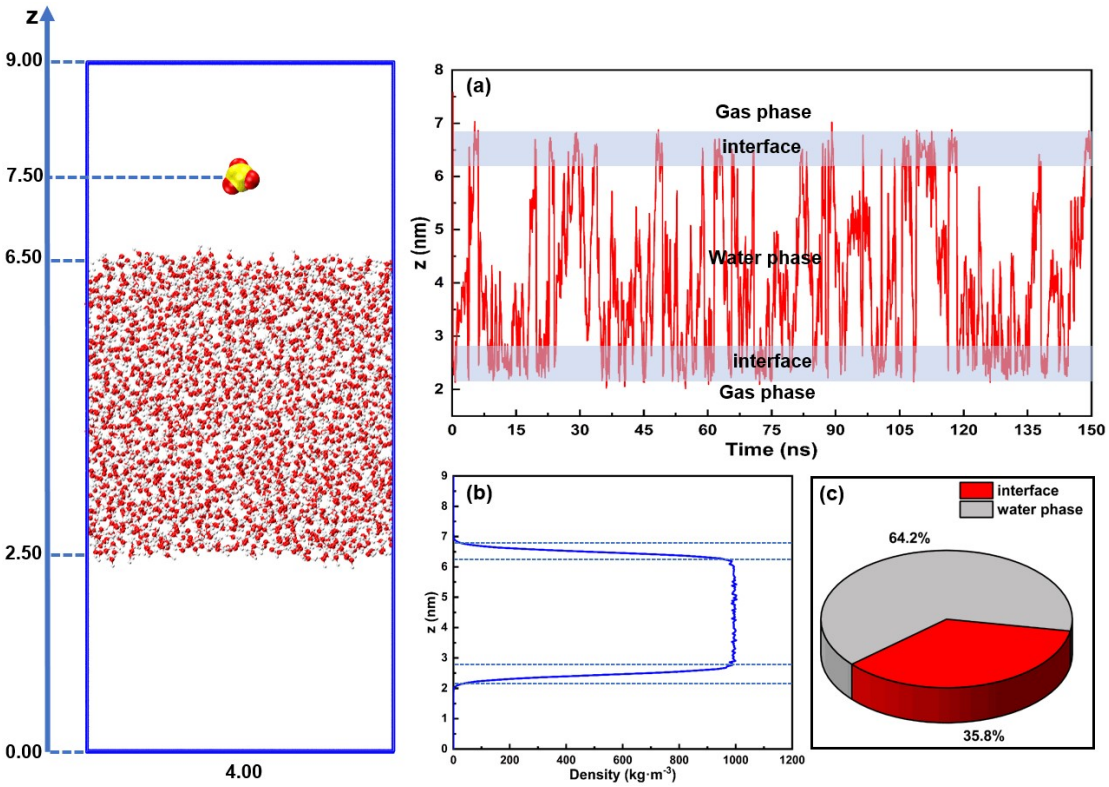

Fig. S7 The z coordinates of SO_3 as the function of simulation time (a) the z coordinates of SO_3 molecule as the function of simulation time; (b) the density profile of water and (c) the pie chart with the occurrence percentages of SO_3 molecule at the air-water interface and in water phase

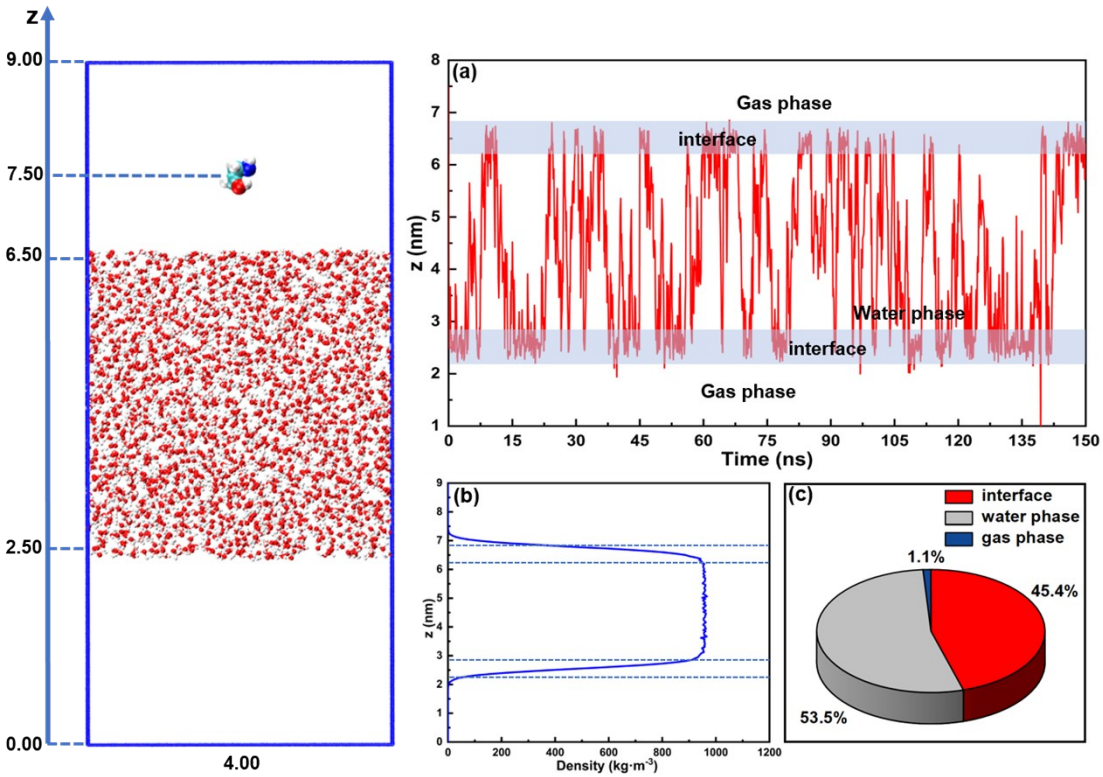

Fig. S8 The z coordinates of MEA as the function of simulation time (a) the z coordinates of MEA molecule as the function of simulation time; (b) the density profile of water and (c) the pie chart with the occurrence percentages of MEA molecule at the air-water interface, in water phase and gas phase

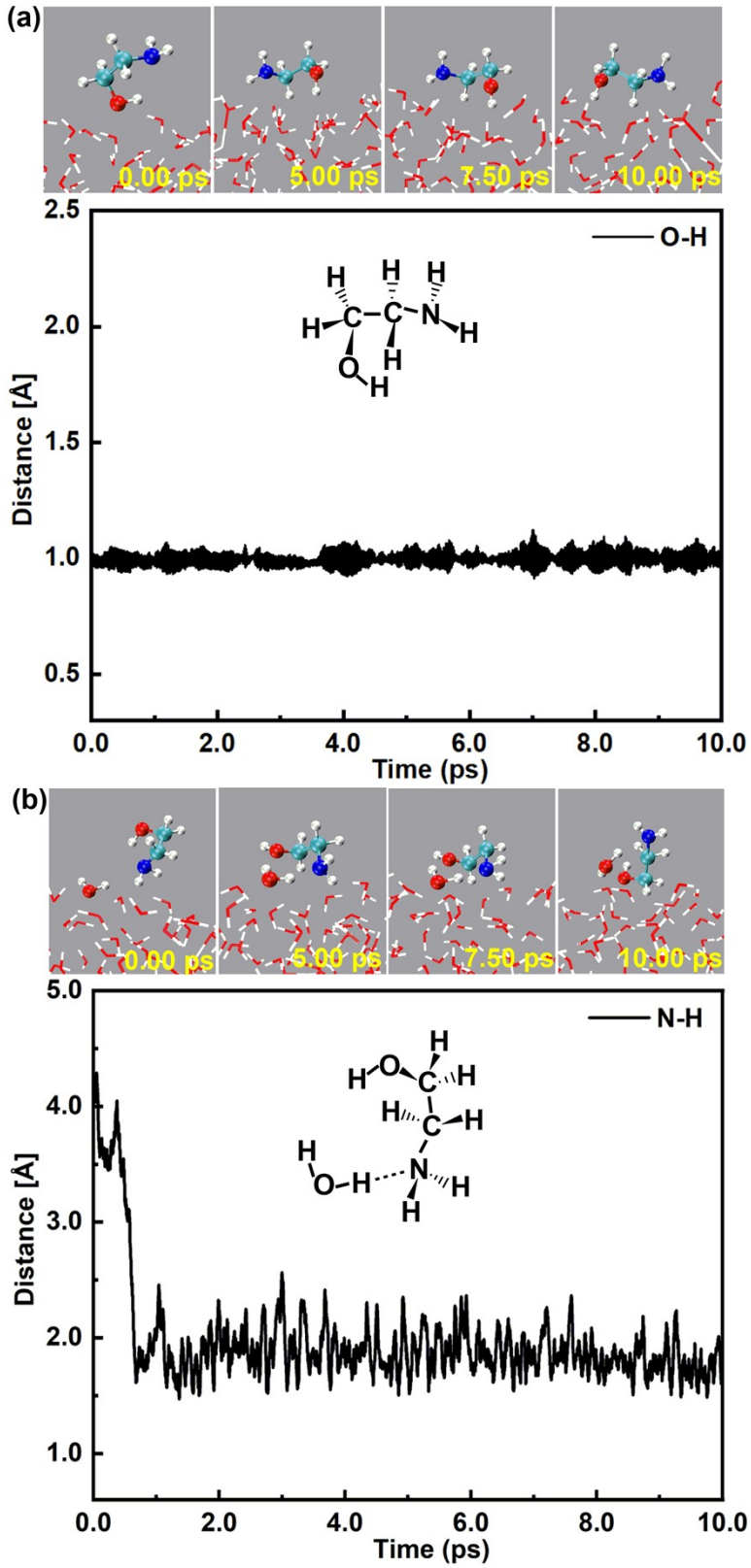

Fig. S9 The simulated trajectories of the formation of $HOCH_2CH_2NH_2$ and $NH_2CH_2CH_2OH$ molecules on water droplet (The white, red, yellow, cyan, and blue spheres represent H, O, S, C and N atoms, respectively.)

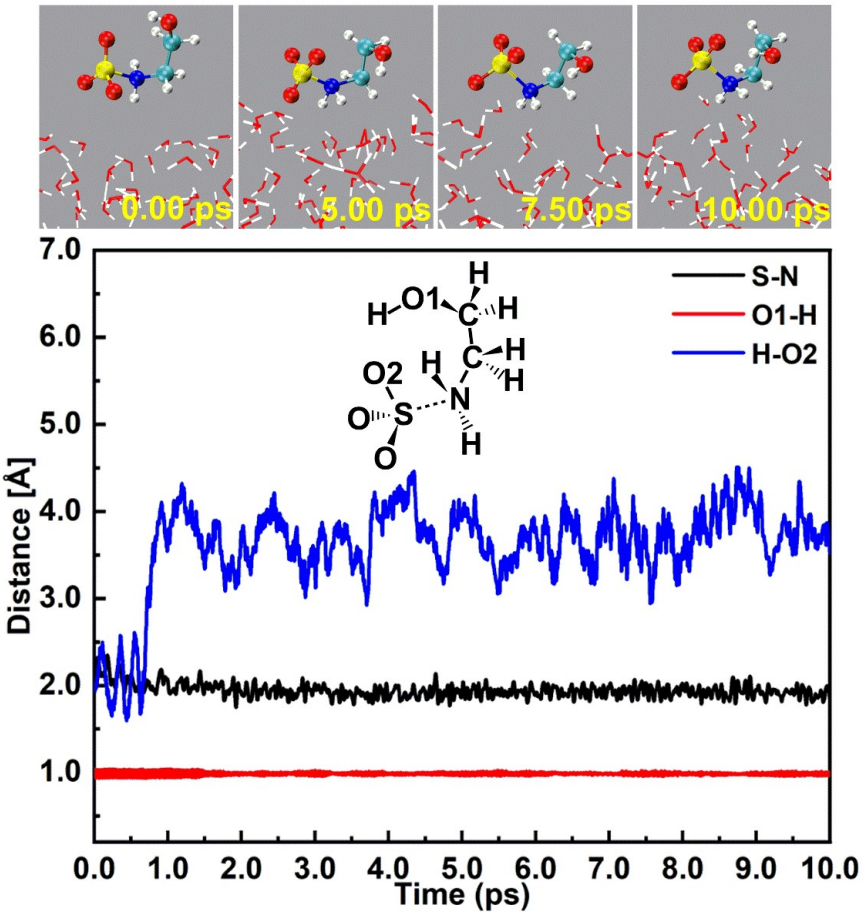

Fig. S10 The simulated trajectories of the formation of SO_3-$NH_2CH_2CH_2OH$ molecule on water droplet (The white, red, yellow, cyan, and blue spheres represent H, O, S, C and N atoms, respectively.)

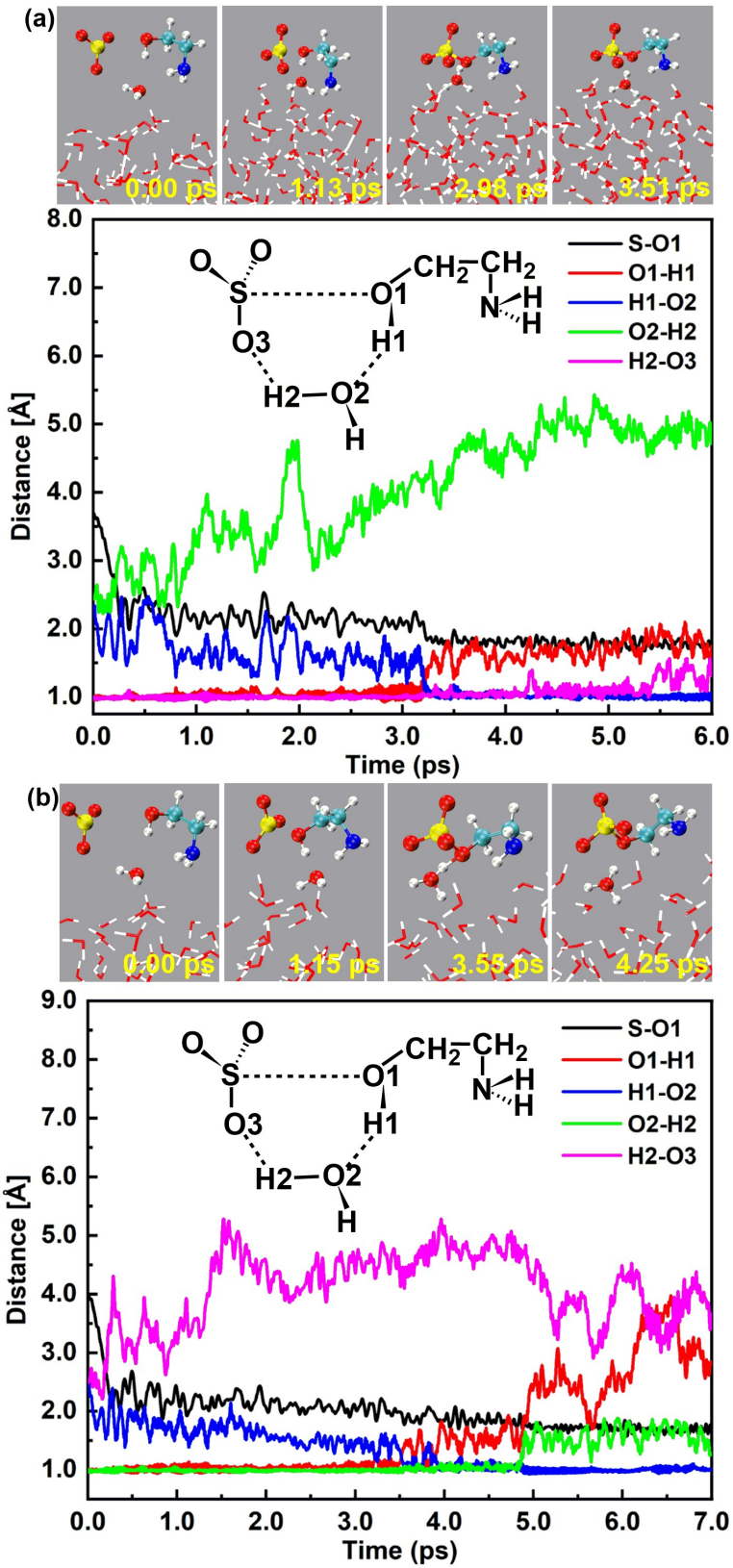

Fig. S11 BOMD simulation trajectories and snapshots of $NH_2CH_2CH_2SO_4^-\cdots H_3O^+$ ion pair from the reaction between SO_3 and $HOCH_2CH_2NH_2$ with one interfacial water molecule on water droplet (The white, red, yellow, cyan, and blue spheres represent H, O, S, C and N atoms, respectively.)

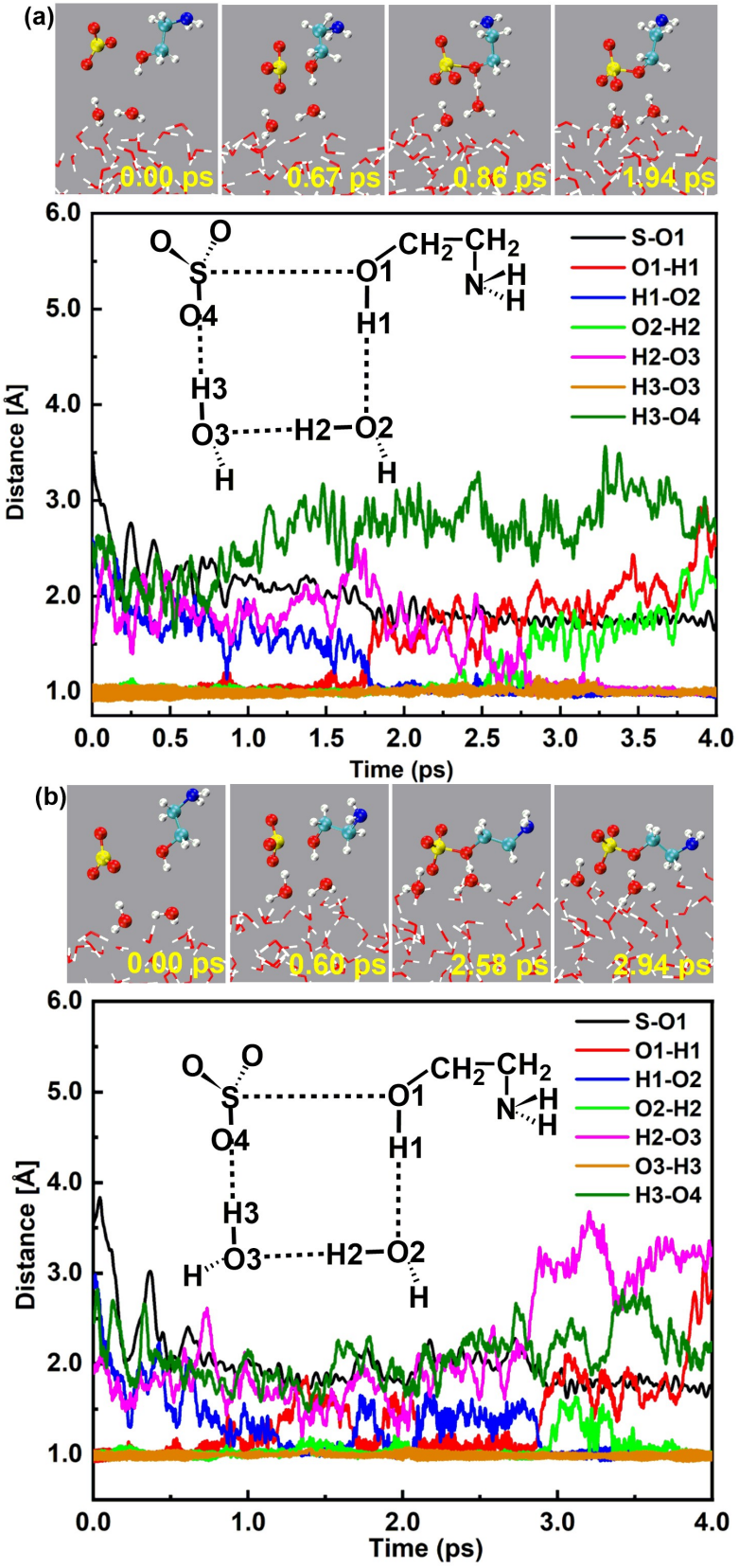

Fig. S12 BOMD simulation trajectories and snapshots of $NH_2CH_2CH_2SO_4^-\cdots H_3O^+$ ion pair from the reaction between SO_3 and $HOCH_2CH_2NH_2$ with two interfacial water molecules on water droplet (The white, red, yellow, cyan, and blue spheres represent H, O, S, C and N atoms, respectively.)

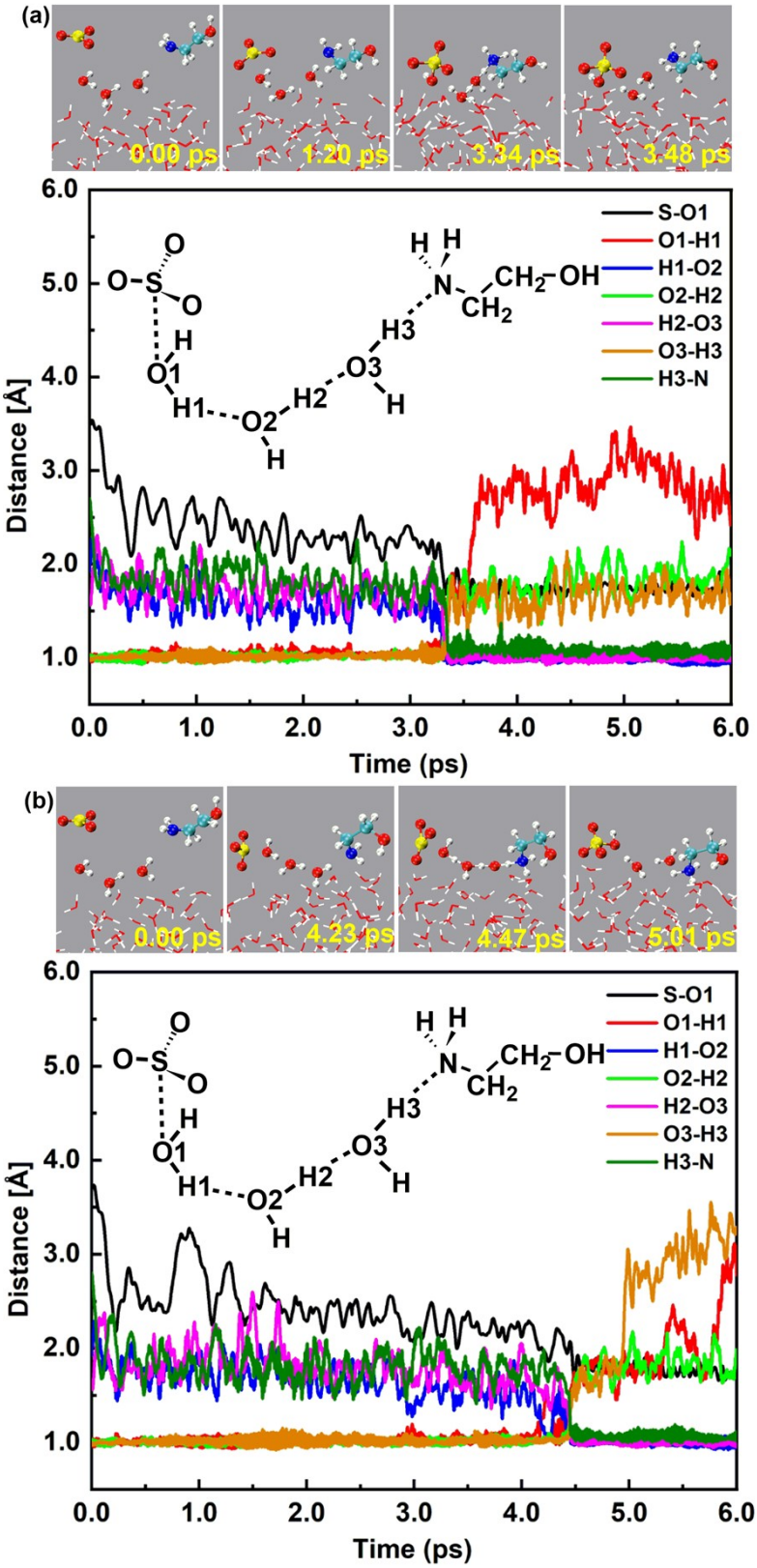

Fig. S13 BOMD simulation trajectories and snapshots of HSO_4^- and $HOCH_2CH_2NH_3^+$ ion from SO_3, $HOCH_2CH_2NH_2$ and three interfacial water molecules on water droplet (The white, red, yellow, cyan, and blue spheres represent H, O, S, C and N atoms, respectively.)

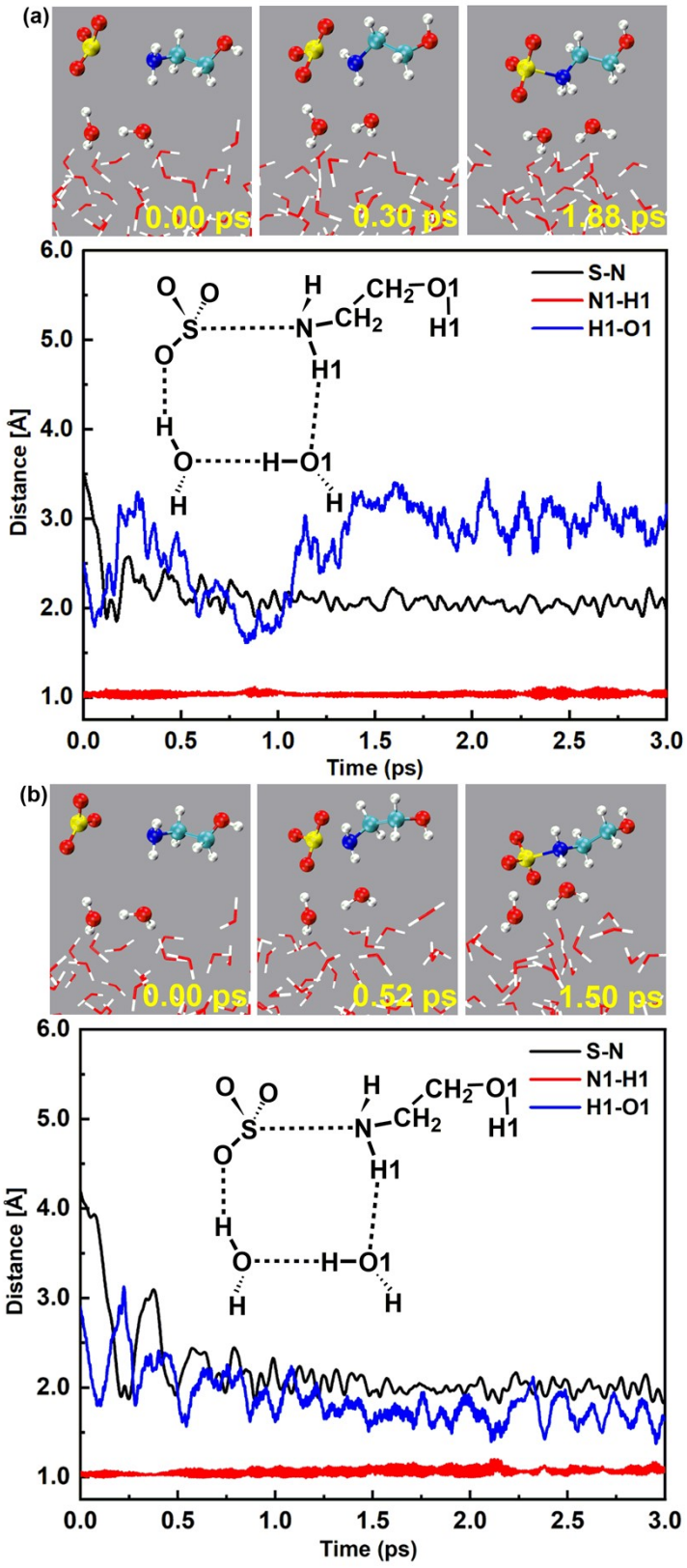

Fig. S14 BOMD simulation trajectories and snapshots of $HOCH_2CH_2NH_2^+$-SO_3^- ion pair from the reaction between SO_3 and $HOCH_2CH_2NH_2$ on water droplet (The white, red, yellow, cyan, and blue spheres represent H, O, S, C and N atoms, respectively.)

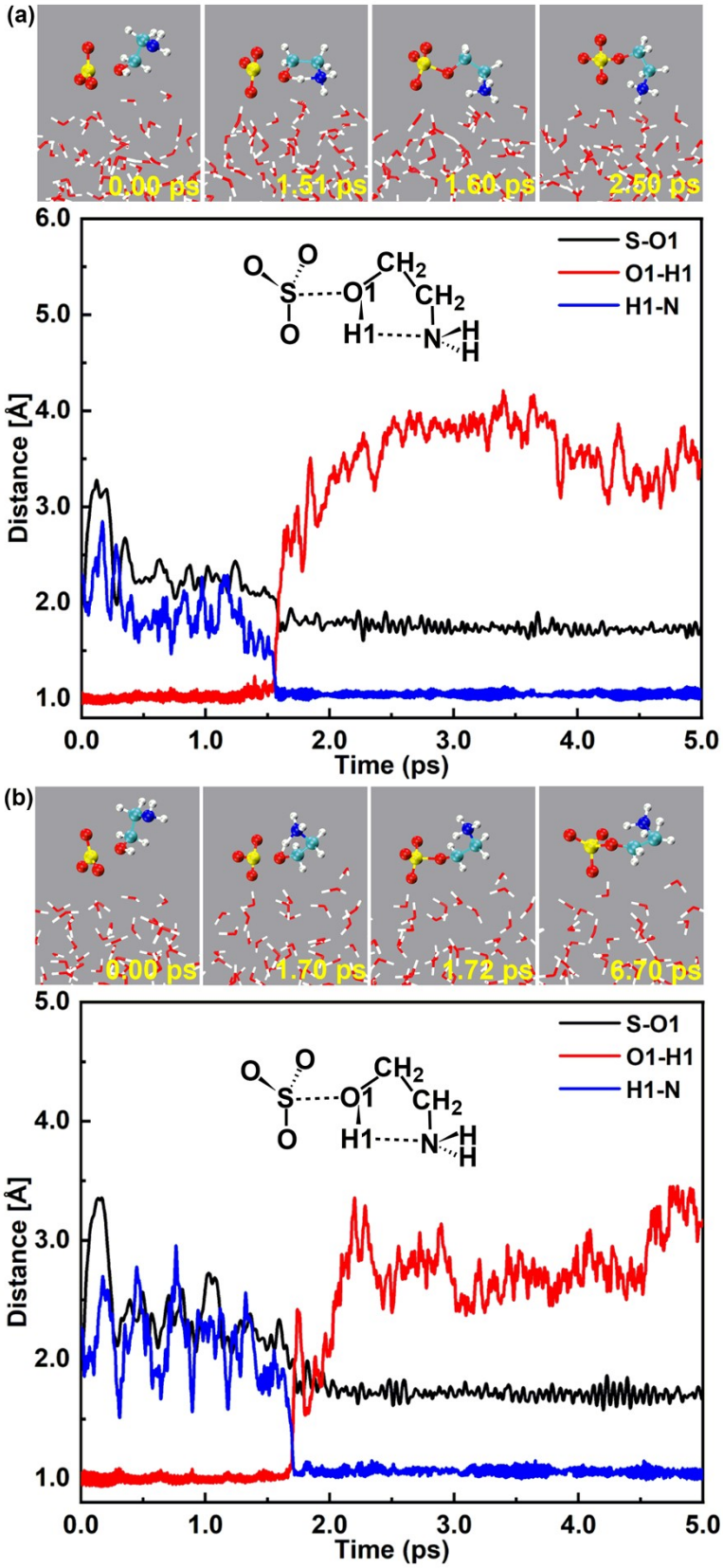

Fig. S15 BOMD simulation trajectories and snapshots of SO_3^--$OCH_2CH_2NH_3^+$ ion pair from the SO_3-$HOCH_2CH_2NH_2$ complex on water droplet (The white, red, yellow, cyan, and blue spheres represent H, O, S, C and N atoms, respectively.)

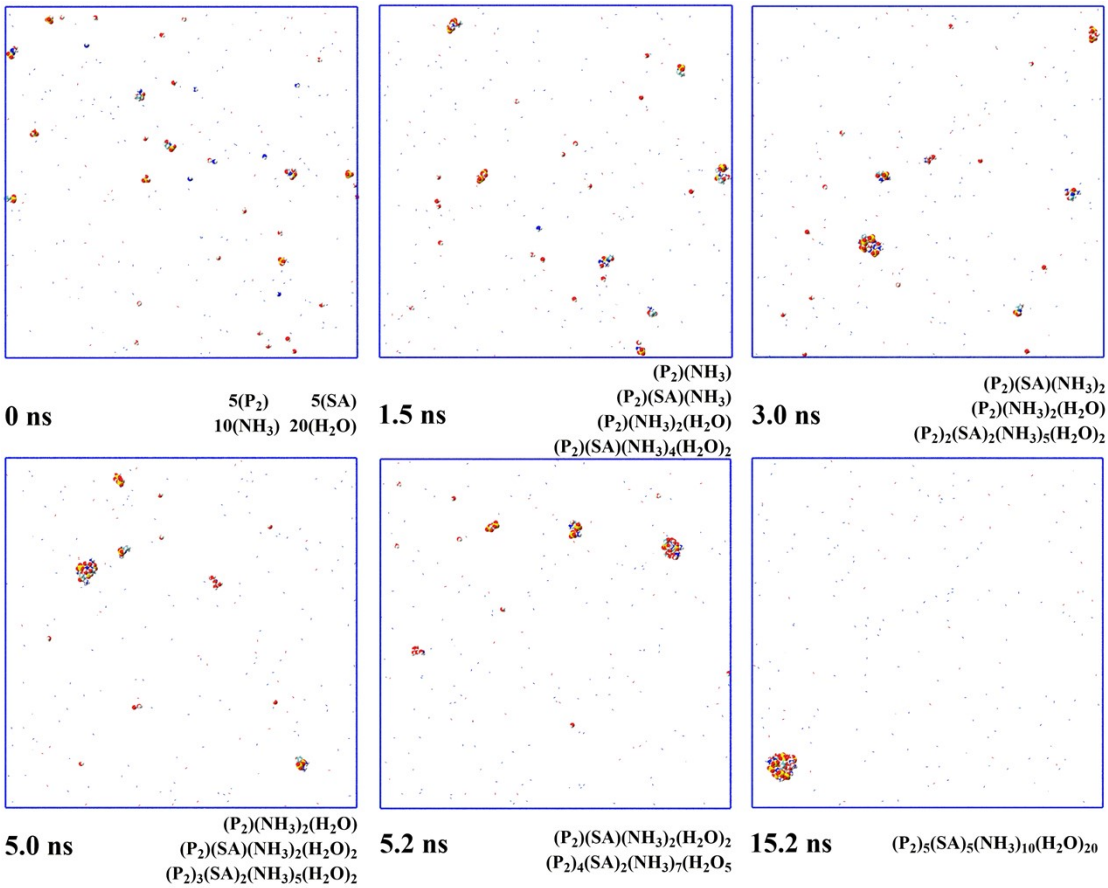

Fig. S16 Snapshots of the nucleation simulation from the product of reaction of SO_3 with NH_2 moiety of $HOCH_2CH_2NH_2$